Research on the Optimization of Blanking Process for the Circuit Breaker Positioning Plate

Qingchun Zheng, Jiaqi Liu, Jingna Liu *, Peihao Zhu, Wenpeng Ma, Zhongyu Gao.

***Abstract*—This paper, through the theory of multi-objective parameter optimization, the finite-element analysis and central composite test of the blanking process of the locating plate of the breaker are carried out. The optimal blanking process parameters of the positioning plate of the circuit breaker are determined, and the influence laws of the independent variable blanking gap, the punch edge radius and the blanking speed on the maximum blanking force and the length of the bright belt are obtained. The experimental results show that the production efficiency of the positioning plate of the circuit breaker is increased by 25%, and the actual machining error is only 4%, which provides a certain guiding significance for optimizing the blanking process parameters.**

***Index Terms*—Center compound test, Multi-objective optimization, Response surface, circuit breaker positioning plate**

I. Introduction

THE circuit breaker positioning plate is the core component of the circuit breaker actuator [1-2]. When the circuit system is overloaded or short-circuited, it can not only provide the energy required for the opening and closing of the circuit breaker [3-4], but also resist the damage to other components caused by the overload impact [5]. Besides, the circuit breaker positioning plate is a blanking product, and the quality of the punching process will seriously affect the quality of the circuit breaker positioning plate. At present, there is a lack of scientific blanking theory and process optimization strategy in the blanking process of circuit breaker positioning plate, resulting in high processing energy consumption and low yield [6-7], which seriously restricts the benign development of blanking process [8-10]. Therefore, it is of great significance to study the blanking theory of the circuit breaker positioning plate and determine the optimal parameters of the blanking process.

In recent years, scholars have carried out much research on sheet blanking from the aspects of practical design and theoretical numerical simulation. Li [11] used mathematical analysis method to analyze the law of blanking crack and propagation in the blanking process of aluminum alloy sheet, and optimized the blanking process combination parameters. NA [12] compared the influences of die clearance angle and die opening size on blanking accuracy and quality, which showed that punch wear is the largest in the initial stage of the stamping process and reasonable clearance can improve processing quality and extend conclusion of tool life. Hatanaka [13] used the finite-element method to simulate the blanking processing technology and pointed out that the length of the bright section to the section is the main impact factor to the quality of the section. Choi [14] studied the effects of blanking clearance and blanking angle on the quality of the section during the blanking process of DP980. Le [15] studied the relationship between the cutting edge quality of AA6111-T4 aluminum alloy plate and the blanking angle and blanking clearance. Hu [16] explored the relationship between blanking clearance and burr height of AA6111-T4 aluminum alloy plate through simulation and studied the mechanism of chip and burr generation on this basis.

Cheon [17] carried out a finite element simulation analysis of crack initiation and propagation during the blanking deformation of metal materials based on the nodal separation technology and proved the consistency between the blanking force-bunching die stroke curve and blanking experimental values. Tekiner [18] used the practical method to conduct blanking experiments for materials with different material thicknesses and proved that the blanking clearance has a significant influence on the burr and blanking force. Cristian [19] used the experimental method to design the AA5754 aluminum alloy sheet blanking process experiment and found that the burr formed during the blanking process of the sheet increased with the increase of the gap. Onur [20] used the Lemaitre damage model to describe the initiation and

Manuscript received March 03, 2021; revised August 15, 2021. This work was supported in part by the National Natural Science Foundation of China (Grant No.62073239 and 61941305), the Science and Technology Program Project of Tianjin (Grant No.19YFFCYS00110) and the Natural Science Foundation of China under Grant No. 6197023003).

Qingchun Zheng is a Professor in the Tianjin Key Laboratory for Advanced Mechatronic System Design and Intelligent Control, School of Mechanical Engineering, Tianjin University of Technology, Tianjin300384, China. (e-mail: zhengqingchun@tjut.edu.cn).

Jiaqi Liu is a postgraduate student in the Tianjin Key Laboratory for Advanced Mechatronic System Design and Intelligent Control, School of Mechanical Engineering, Tianjin University of Technology, Tianjin300384, China. (e-mail: liujiaqi0921@163.com).

Jingna Liu is a Lecturer in the Tianjin Key Laboratory for Advanced Mechatronic System Design and Intelligent Control, School of Mechanical Engineering, Tianjin University of Technology, Tianjin300384, China. (corresponding author, phone: (+86)13821826079; e-mail: liujingna2003@163.com).

Wenpeng Ma is a Lecturer in the Tianjin Key Laboratory for Advanced Mechatronic System Design and Intelligent Control, School of Mechanical Engineering, Tianjin University of Technology, Tianjin300384, China. (e-mail: wenpengma@sina.com).

Peihao Zhu is an Associate Professor in the Tianjin Key Laboratory for Advanced Mechatronic System Design and Intelligent Control, School of Mechanical Engineering, Tianjin University of Technology, Tianjin300384, China. (e-mail:zhupeihao-gp@163.com).

Zhongyu Gao worked as an assistant engineer in the Tianjin Nano Machinery Manufacturing Co., Ltd Tianjin 300462, China. (e-mail: 77854952@qq.com).

propagation of punching cracks. The optimal punching gap is obtain by analysis, and simulation values are close to the experimental values. Seunghyeon [21] designed a program for predicting the service life of blanking dies and carried out blanking experiments. The error between the experimental value and the theoretical calculation value is only 7.2%.

In general, above research lacks the research and formulation of blanking theory and process optimization strategies related to the processing of circuit breaker protectors. They only used the single factor method and the orthogonal test method, and did not consider the multi-objective optimization of the bright band and the blanking force. Therefore, the resulted high processing energy consumption and low yield had incredibly restricted the development of the blanking process. This paper uses the finite element method, centre compound experiment and multi-objective optimization to study the influence of independent variable blanking clearance, punch edge radius and blanking speed on the maximum blanking force and the length of the bright belt, determines the best blanking process parameters of the positioning plate and realizes the scientific process of positioning plate blanking. What's more, the blanking theory and technology of the circuit breaker positioning plate are improved, and problems of high energy consumption and low power in actual production are solved.

II. MULTI - OBJECTIVE OPTIMIZATION THEORY AND METHOD

A. Response surface analysis and experimental design principles

Response surface analysis [22-23] is a method to seek the optimal combination of test factors and obtain the optimal target value through experimental designs. The mathematical expression can be get by

$$y = \alpha f'(x) + \beta \tag{1}$$

Where x is the transpose of the vector $(x_1, x_2, ..., x_n)$, $f(x)$ is the m-dimensional response function matrix, the orthogonality and transposability are satisfied. α is the unknown parameter vector, and β is the appropriate modifier.

Response surface method is used to establish the mapping relationship between maximum blanking force, length of bright band and parameters. The commonly used models in the response surface method are the first-order response surface model and the second-order response surface model. Due to the nonlinear relationship between the maximum blanking force, the length of the bright band and the three parameters, the first-order response surface model cannot satisfy the regression effect. Therefore, this paper adopts a second-order response surface model to establish the blanking model of positioning plate of the circuit breaker. The second-order response surface model [24-25] can be expressed by

$$\hat{y} = \alpha_0 + \sum_{i=1}^{N} \alpha_i x_i + \sum_{j=1}^{N} \alpha_j x_j^2 + \sum_{ij(i<j)}^{N} \alpha_{ij} x_i x_j \tag{2}$$

Where $\hat{y}$ is the response predicted by the approximate model, x is the design variable, N is the number of variables, and α is the undetermined coefficient [26-27], which is determined by

$$\alpha = \left(X^{\mathrm{T}} X\right)^{-1} X^{\mathrm{T}} y \tag{3}$$

Where X is the experimental sample point matrix, X^T is the transposed matrix of x, and y is experimental observation vector.

The principle of the central composite test design is composed of three parts: cubic point, axial point and central point test in space, which is shown in Fig 1.

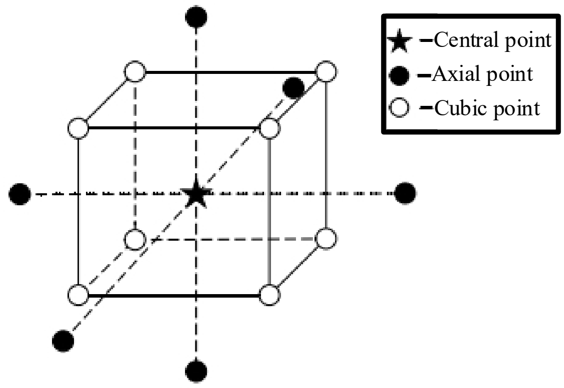

Fig. 1 Schematic diagram of CDD principle

The cube point is the point at every point of the cube, and the axial point is the point on the coordinate axis established by the center of the cube. The factor selection of the axial point is determined by the value of α, which is calculated by the formula (4). In the design of central composite test, the value of parameters will be taken out of the predetermined parameter space according to the size of α, which is convenient for exploring the parameter space outside the sample.

$$\alpha = 2^{\frac{k}{4}} \tag{4}$$

Where k is the number of factors tested.

B. Multi-objective genetic algorithm

Multi-objective optimization problem refers to the optimization problem when many factors and objectives need to be considered in the actual application of engineering. The more detailed the factor and index analysis, the more accurate the model will be. However, the improvement of accuracy often brings a huge amount of calculation and technical difficulties to solve the problem. The multi-objective optimization method can grasp the main contradictions of the problem, eliminate secondary factors and simplify the problem.

In general multi-objective optimization problems, Pareto solutions are usually continuous and have infinite numbers, which is shown in Fig 2. The optimal solution obtained by multi-objective optimization is the result of a trade-off among objectives. The optimal solution may not be the optimal solution for a single objective, but it can be considered as the best solution to achieve each sub-objective as far as possible. In this paper, NSGA-II [28-29] algorithm is used to enhance the ability to select the solution near Pareto and accelerate the acquisition of the optimal solution.

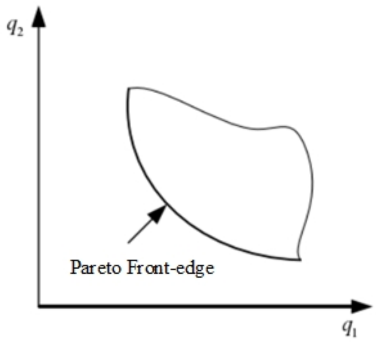

Fig.2 Pareto Front-edge Disassembly

The multi-objective optimization is defined by

$$\min f_m(x), m = 1,2,\dots,M$$
$$s.t.\begin{cases} g_j(x) \le 0, j = 1,2,\dots,J \\ hk(x) = 0, k = 1,2,\dots,K \\ X_i^{(L)} \le X_i \le X_i^{(U)}, i = 1,2,\dots,n \end{cases} \tag{5}$$

Where, X_i is the i variable and N is the total number of design variables; X_i^L and X_i^U is the upper and lower limit of the value of the i design variable. $f_m(x)$ is the m sub-objective function, M is the total number of sub-objective functions, $g_j(x)$ is the j inequality constraints, J is the total number of inequality constraints, $hk(x)$ is the k equality constraints, and K is the total number of equality constraints.

III. FINITE ELEMENT MODEL OF THE BLANKING POSITIONING PLATE

The positioning plate blanking process is divided into four steps: left punch punching, right punch punching, second punch punching, and blanking. The model is Built in Fig.3, and properties of H85 brass is defined according to Table 1.

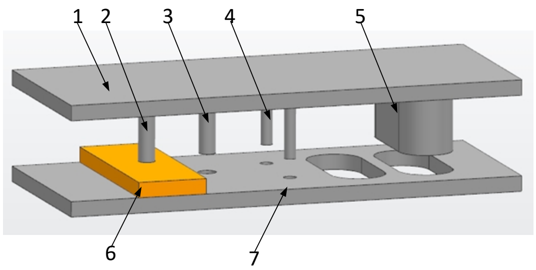

Fig.3. Finite element model1-Punch, 2-first punch left punch, 3-first punch right punch, 4-second punch, 5-punch blanking punch, 6-sheet, 7-die

TABLE I
MAIN PARAMETERS OF SHEET BLANKING MODEL

Material	H85brass
Length(mm)	9
Thickness(mm)	2
Density(kg/m²)	8900
Modulus of elasticity(MPa)	115000
Poisson'sratio	0.34

In ABAQUS, the model is meshed and the finite element model is shown in Fig 4.

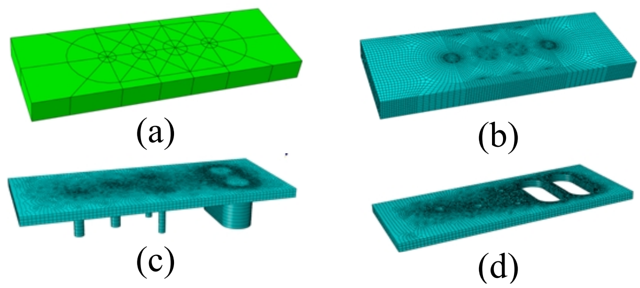

Fig.4. Finite element model:(a) Sheet metal division(b) Sheet metal(c)Punch(d)Die.

The contact between the mold and the sheet is defined as surface-to-surface contact between a rigid body and deformed body. Fixed constraints are set around the sheet and the reference points are placed on the punch and die, thus constraining the movement of the punch and die [30], which is shown in Fig.5.

Fig.5. Motion analysis

According to the actual production analysis, the blanking speed is set to 4mm/s in the Y_D-direction, and the reference point XL is set to be shifted 9mm.to the left. The analysis steps and movements are set as shown in Table 2.The impact of different blanking speeds on forming can be analyzed by changing the blanking speed of the punch.

TABLE 2
ANALYSIS STEPS AND LOAD SETTINGS

Step	Mould horizontal moving speed (mm/s)	Punch blanking speed (mm/s)	Time (s)
1	0	4	2.5
2	360	0	0.025
3	0	4	2.5
4	360	0	0.025
5	0	4	2.5
6	360	0	0.05
7	0	4	2.5

Based on the above, the ABAQUS analysis model of the positioning plate progressive mold is completed. According to the actual production of the company, the blanking speed of the simulation is set as 4mm/s, the blanking clearance is set as 0.18mm, and the fillet radius of the punch edge is set as 0.5mm.

The maximum stress is 362.7MPa after the first punching (a) and 385.6MPa after the second punching (b). In general, the stress increases significantly. When the stress reaches 295MPa between the two holes, plastic deformation will occur. This is because the distance between the two holes is relatively close, and the first hole has a more significant impact on the punching of the second hole, so the two holes cannot be punched at the same time. If the two holes are punched at the same time, fracture will occur between the two holes. The third process (c) has a large spacing between the two holes, so that it can be punched simultaneously. The maximum stress is 390.2MPa. The fourth process (d) has the same maximum stress as the third process and the maximum stress is 397.3MPa,which is shown in Fig.6.

Based on the constitutive model of H85 brass, a simulation model of progressive die blanking for the circuit breaker positioning plate is established. The impact of blanking speed, blanking clearance and fillet radius of punch edge on the length of the bright band and blanking force are determined.

A. Impact of blanking clearance on length of the bright band and blanking force

The controlled variable method is used to study the relationship between the blanking gap and the length of the bright band of the brass blanking section and the blanking force. Setting the blanking speed as 4mm/s, the fillet radius of punch edge as 0.5mm, and the blanking clearance as 0.07mm, 0.13mm, 0.18mm, 0.23mm, 0.28mm is to simulate the positioning plate punching process. The length of the bright band is shown in Figure 7.

It can be seen from Fig.8 that as the blanking clearance increases, the length of the bright band and the maximum blanking force show a decreasing trend, where the optimal blanking clearance is selected as 0.18mm.

B. Impact of fillet radius of punch edge on length of the bright band and blanking force

The control variable method is used to explore the relationship among the radius of the punch edge fillet, the length of the bright band of the brass blanking section and the blanking force. The blanking speed is set as 4mm/s, the blanking clearance is set as 0.18mm. Then, the finite element simulation of the blanking process of the circuit breaker positioning plate is performed, and the relationship among the fillet radius of the cutting edge of the different punches, the length of the bright belt and the blanking force is obtained, and the result is shown in Fig.9.

It can be seen from Fig.9 that the length of the bright band increases first and then decrease with the increase of fillet radius of punch edge. In addition, the maximum blanking force increases gradually. Meanwhile, the increase of fillet radius results in more burrs and collapse angles of the punching section, and the optimal fillet radius of the punch edge is 0.5mm.

C. Impact of blanking speed on length of bright band and blanking force

In the same way, the blanking clearance is set as 0.18mm, and fillet radius of punch edge is set as 0.5mm. Finite-element simulation about the blanking process of the circuit breaker positioning plate is carried out to find out the relationship between blanking speeds and the length of bright band as well as blanking force, which is shown in Fig 10.

It can be seen from Fig.10 that the length of the bright band shows an increasing trend with the continuous increase of blanking speed. Though the impact of blanking speed on blanking force is small, the overall trend is decreasing. Excessive blanking force will result in faster wear of punch and may cause unpredictable damage to the machine tool. Therefore, the optimal blanking speed is selected as 5mm/s.

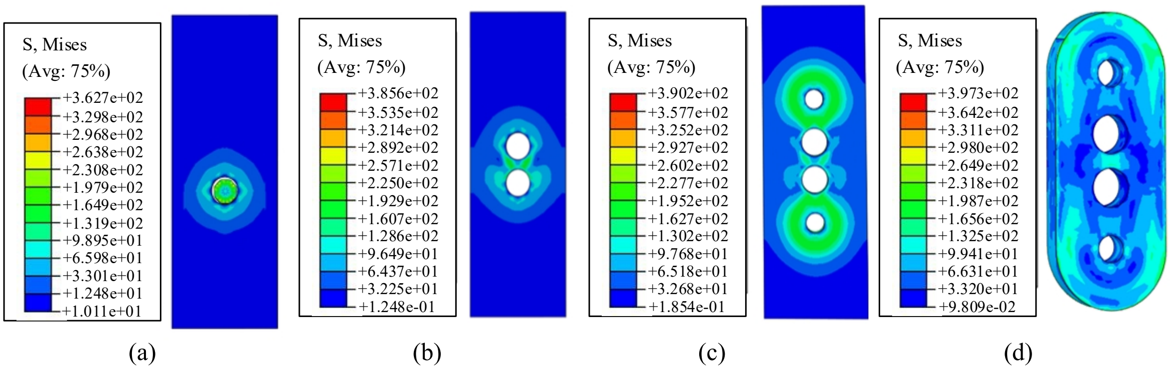

Fig.6. Strain simulation results: (a) The first step state (b) The second step state (c) The third step state (d) The fourth step state

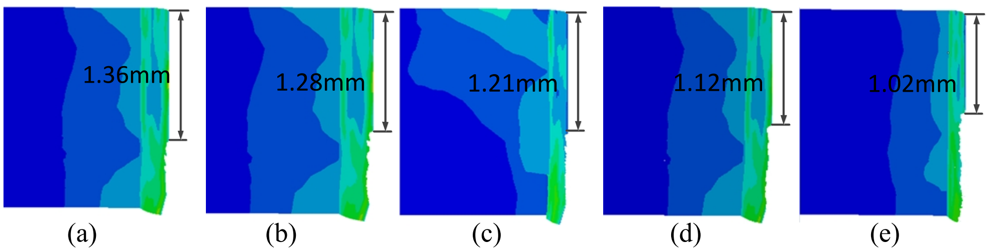

Fig. 7 Analog values of bright band lengths at different blanking intervals(a) Blanking clearance is 0.07mm (b) Blanking clearance is 0.13mm (c) Blanking clearance is 0.18mm(d) Blanking clearance is 0.23mm(e) Blanking clearance is 0.28mm.

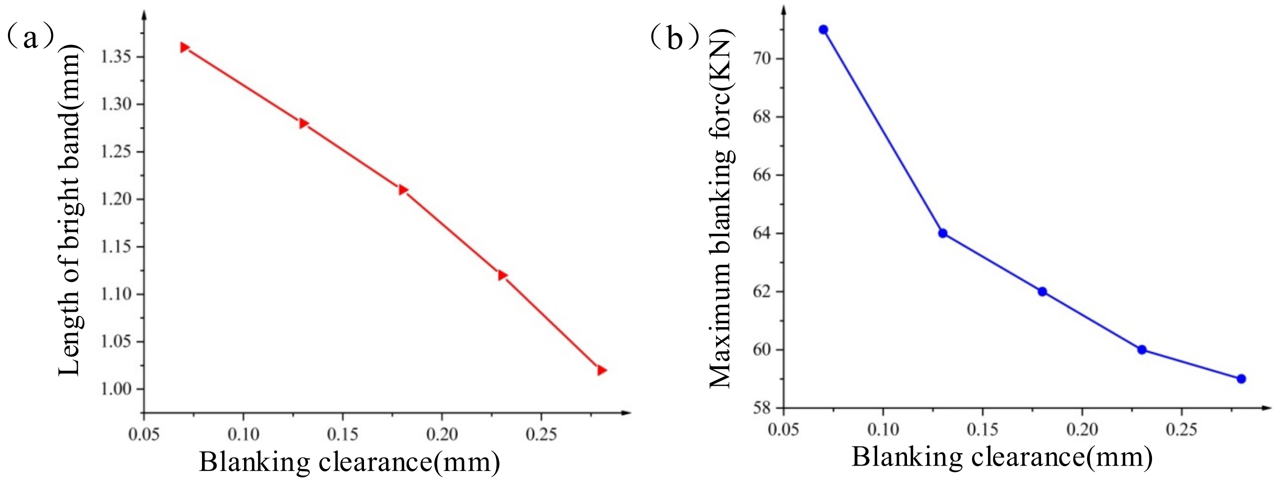

Fig.8. (a) Influence of blanking clearance on the length of the bright band and (b) Influence of blanking clearance on maximum blanking force.

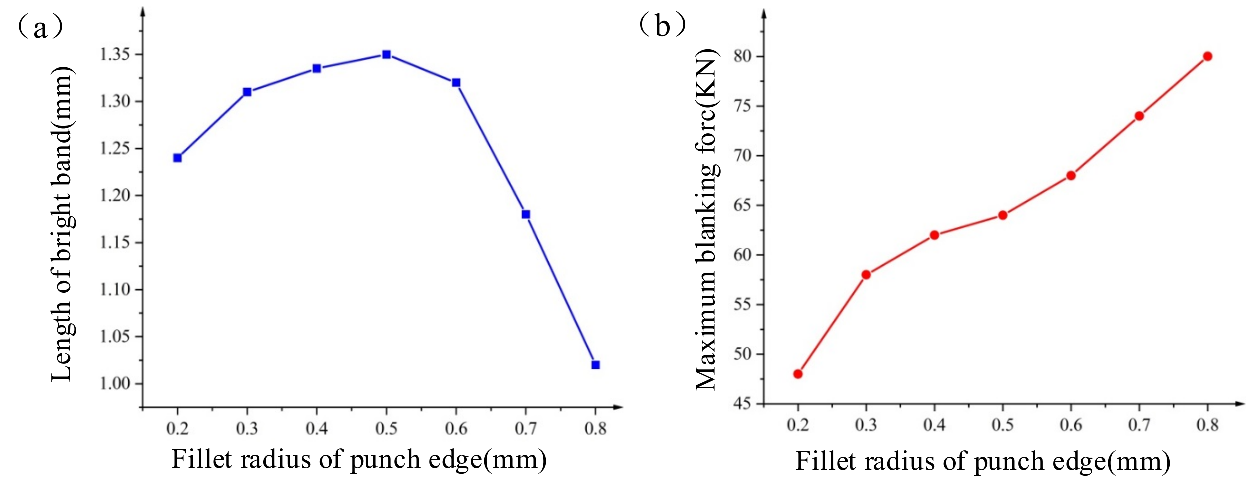

Fig.9. (a) Influence of fillet radius of punch edge on the length of the bright band and (b) Influence of fillet radius of punch edge on maximum blanking force.

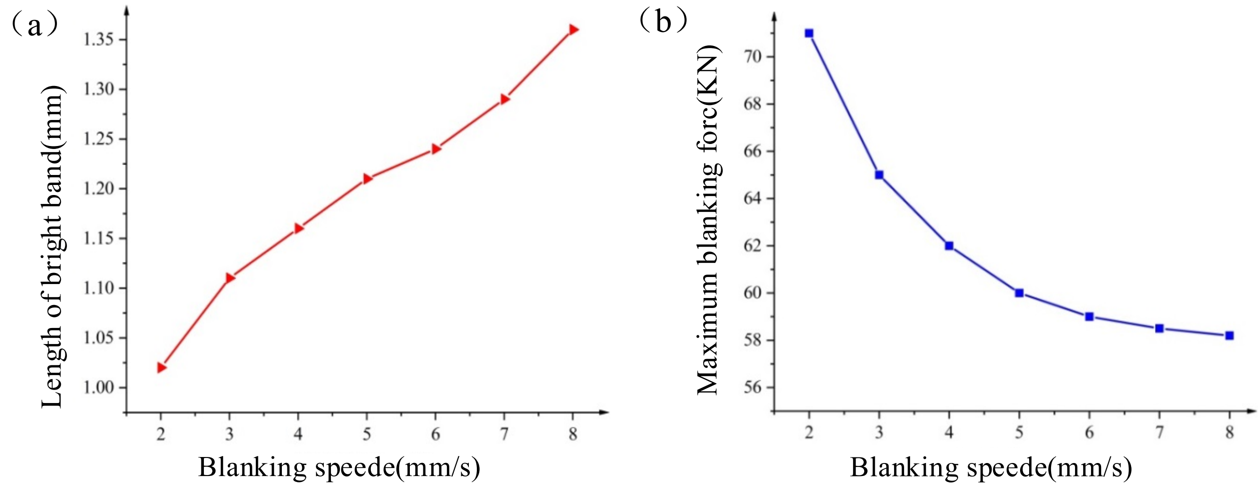

Fig.10. (a) Influence of blanking speed on the length of the bright band and (b) Influence of blanking speed on maximum blanking force.

D.Blanking response model and optimization

The blanking clearance, fillet radius of punch edge and blanking speed are the main factors that decide the blanking quality of the circuit breaker positioning plate. Response surface model [31-32] is built with these three parameters used as the influencing parameters for center compound experiment [33]. In addition, the variation range of each parameter is measured during the blanking of positioning plate. The actual production process parameter range is defined by Tianjin Jinrong Tianyu Precision Machinery Co., Ltd. The range of blanking clearance is set from 0.08 to

0.24mm, the range of fillet radius of punch edge is set from 0.3 to 0.84mm and the range of punching speed is set from 1.64 to 8.36mm/s.

Two parameters with a high reference value for blank forming should be selected as the optimization target for the central composite design method. In this study, the length of the bright band and the maximum blanking force are selected as the target variables. In addition, blanking clearance x1, fillet radius of punch edge x2 and blanking speed x3 are used as independent variables. Central composite design parameters shown in Table 3 are obtained.

TABLE 3.
TEST PARAMETERS OF RESPONSE SURFACE MODEL

Group	Blanking clearance x_1 (mm)	Fillet radius of punch edge x_2(mm)	Blanking speed x_3(mm/s)	Length of bright band y_1(mm)	Maximum blanking force y_2(KN)
1	0.28	0.50	5.00	1.40	58.5
2	0.18	0.50	5.00	1.45	61.5
3	0.18	0.50	5.00	1.45	61.5
4	0.12	0.30	3.00	1.41	63.0
5	0.12	0.70	7.00	1.53	63.5
6	0.12	0.30	7.00	1.27	58.0
7	0.24	0.30	3.00	1.30	61.5
8	0.18	0.50	8.36	1.42	61.5
9	0.08	0.50	5.00	1.35	62.0
10	0.12	0.70	3.00	1.40	63.0

The process optimization of positioning plate blanking studied in this paper is a problem of optimizing the design of two or more targets at the same time. In order to obtain the mapping relationship, Design-Expert is used to perform a second-order response surface linear regression on the variables in Table 4 [34-36].The optimal solution obtained may not be the optimal solution of a single goal, but it is the solution that makes each sub-goal reaches the optimal solution as far as possible.

The regression formula of the prediction model can be expressed by

$$\begin{aligned} y_1 &= 0.3406 - 0.0849x_1 + 0.9064x_2 + 0.0188x_3 + 0.3125x_1x_2 \\ &+0.0729x_1x_3 + 0.0593x_2x_3 - 2.7196x_1^2 - 1.2612x_2^2 - 0.0038x_3^2 \end{aligned} \tag{6}$$

The second-order response surface linear regression of independent and dependent variables in Table 4 is performed by Design-Expert.

A three-dimensional map composed of the length of the bright band and the influencing parameters of the positioning plate forming can directly reflect the influence of each variable on the response variable. The impact of the independent variable on the length of the bright band is shown in Fig.11.

A second-order response surface linear regression is performed between the independent variables and dependent variable in Table 4 using the same method. The regression formula of the prediction model is described in formulas (7). The effect of the independent variable on the maximum blanking force is shown in Fig.12.

$$\begin{aligned} y_2 &= 184.3917 + 163.8997x_1 - 11.6237x_2 - 30.7373x_3 \\ &-52.0833x_1x_2 + 15.6250x_1x_3 + 35.9375x_2x_3 - 985.9439x_1^2 \\ &-93.1544x_2^2 + 0.6595x_3^2 \end{aligned} \tag{7}$$

Isight performs multi-objective optimization to obtain all Pareto solution sets. Partial Pareto solutions are shown in Table 4. In the sight window, the scatter diagram between the bright band length, the maximum blanking force and the independent variable can be observed, as shown in Fig.13(a). The highlighted points in the figure are the scattered points of Pareto optimization solution on the coordinate axis. Fig.13(b) shows the distribution of Pareto optimization solution set on 3D coordinate axis.

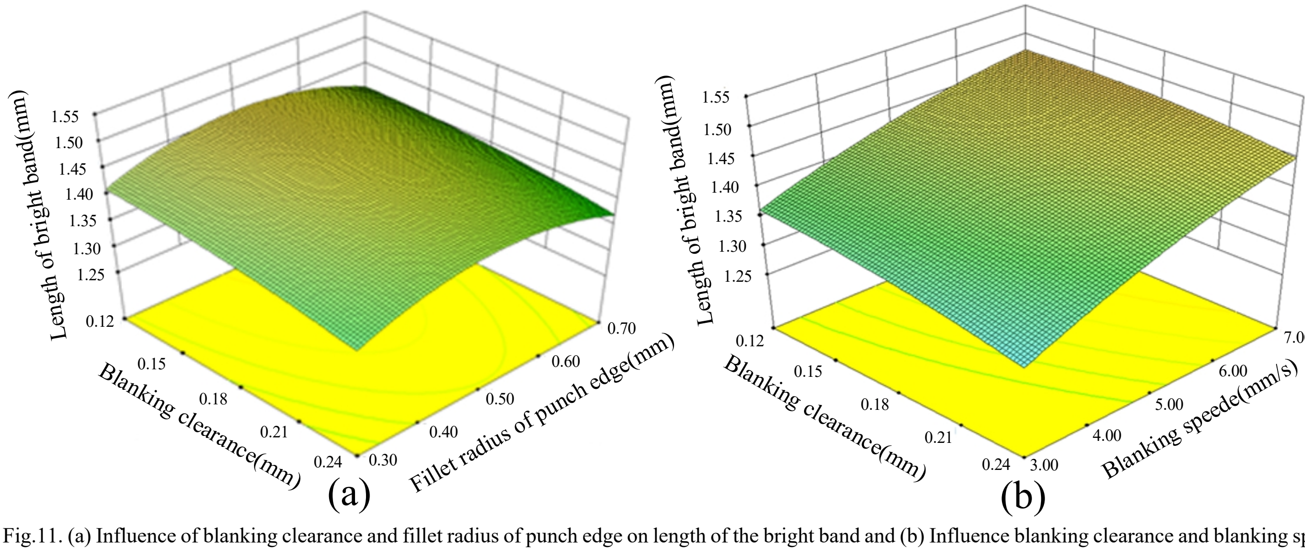

Fig.11. (a) Influence of blanking clearance and fillet radius of punch edge on length of the bright band and (b) Influence blanking clearance and blanking speed on length of the bright band

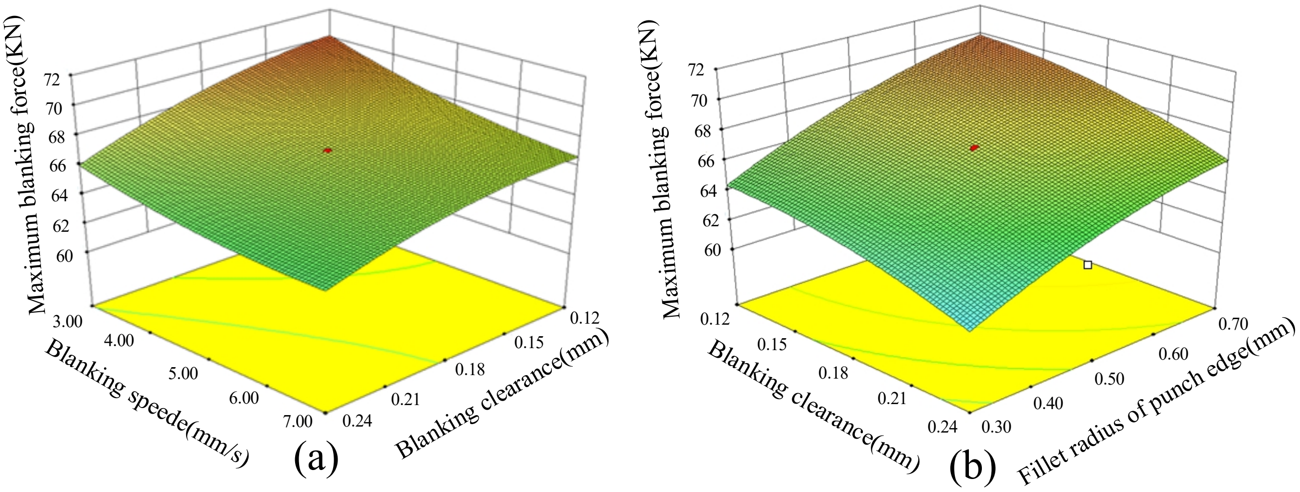

Fig.12. (a) Influence of blanking clearance and fillet radius of punch edge on maximum blanking force and (b) Influence of blanking clearance and blanking speed on maximum blanking force

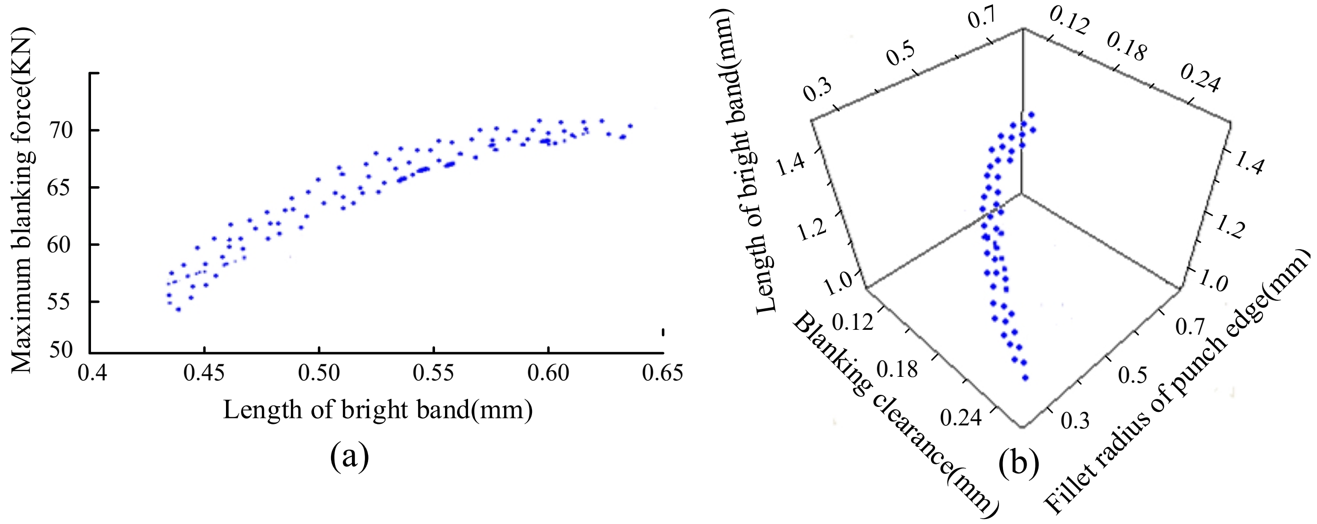

Fig.13 Distribution of optimal solutions: (a) Optimal solution distribution of length of bright band and maximum blanking force and (b) Optimal solution distribution of length of bright band, blanking clearance and punch edge fillet radius t in 3D view.

TABLE 4.
PART OF THE PARETO SOLUTIONS

Group	Blanking clearance x_1 (mm)	Fillet radius of punch edge x_2(mm)	Blanking speed x_3(mm/s)	Length of bright band y_1(mm)	Maximum blanking force y_2(KN)
1	0.17	0.58	4.87	1.42	68.48
2	0.28	0.54	5.05	1.47	65.57
3	0.17	0.49	4.83	1.44	70.75
4	0.18	0.52	5.11	1.42	69.54
5	0.15	0.38	3.57	1.47	70.02
6	0.15	0.41	5.06	1.45	58.48
7	0.19	0.16	5.28	1.15	62.18
8	0.25	0.48	5.28	1.44	59.57
9	0.28	0.47	5.24	1.31	58.43
10	0.13	0.37	7.44	1.04	58.75

Impacts of various factors on the maximum response value are reflected intuitively by the response surface shown in Fig.11, in which the blanking clearance has the largest effect on the length of bright band, i.e., relatively small blanking clearance results in higher force between the metal material and the punch. The fracture of brass is delayed and the bright band of blanking section is increased by means of better exerted plasticity of metal materials and fully suppressed occurrence of blanking cracks. The impact of blanking speed on the length of bright band is small. The length of bright band increases when the blanking speed gets higher. This because that fluidity of the material is improved and the bright band becomes longer at raised speed. The fillet radius of punch edge has the least impact on the length of bright band. As the radius of fillet of punch edge increases, the length of bright band increases first and then decreases.

The impact of blanking clearance, blanking speed and fillet radius of punch edge blanking force are reflected intuitively by the response surface shown in Fig.12. The blanking force decreases as the blanking speed gets higher. When the speed increases to a certain value, the reduction of blanking force is even less noticeable. As the blanking clearance increases, the blanking force gets lower, on the other hand, as the fillet radius of punch edge increases, the blanking force gets higher.

This paper combines the specific data given in Table 4 to analyze the distribution of Pareto's optimized solution set on 2D and 3D coordinate axes. It can be seen that the optimized solution for the blanking clearance is 0.152mm, and the optimal solution of fillet radius of punch edge is 0.41mm, and the optimal solution of blanking speed is 5.06mm/s. In order to facilitate experimental processing, approximate parameters are taken. That is, the blanking clearance is 0.15mm, the fillet radius of punch edge is 0.4mm, and the blanking speed is 5mm/s.

IV. Experimental Verification of the Optimal Solution

Blanking test of Pareto's optimal solution is verified by the progressive mold provided by the enterprise. The part diagram of the positioning plate of the circuit breaker is shown in Fig.14.

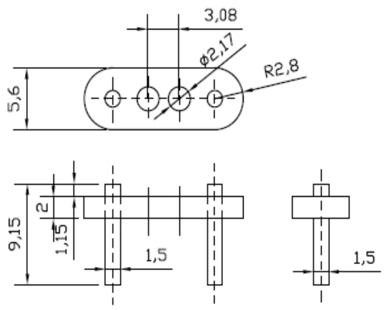

Fig.14. Three views of the positioning plate

In this paper, the NS1-800 punching machine is used for blanking experiment. The maximum height of the stamping die is set as 300 mm, the range of adjustment for the height of stamping die is set as 80 mm, the stroke of the sliding block for the stamping machine is set as 100 mm and the stroke of the sliding block is set as 55-125 times/min. Install the progressive die before connecting the punch pressure sensor to measure the punching force, which is shown in Fig.15. Two-dimensional digital image measuring instrument is used to measure the length of bright belt on the blanking section of the positioning plate. Besides, blanking force is recorded to measure the bright belt's length, which is shown in Fig.16.

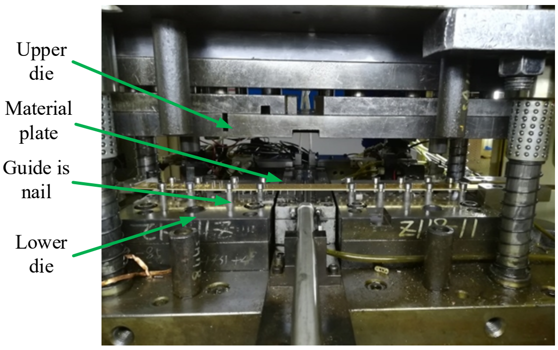

Fig.15. Mold installation

Fig.16. Measuring bright band

Measuring the parameters of the fourth procedure. The maximum blanking force of the product punched out before the improvement of process parameters is 62.7KN and the bright section of the stamping part measured by a two-dimensional digital measuring instrument (Fig.17a) is 1.2mm. The maximum blanking force of the product punched out after the improvement of process parameters is 58.6KN and the length of the bright section of the stamping part is measured by a two-dimensional digital measuring instrument (Fig.17b) is 1.51mm.

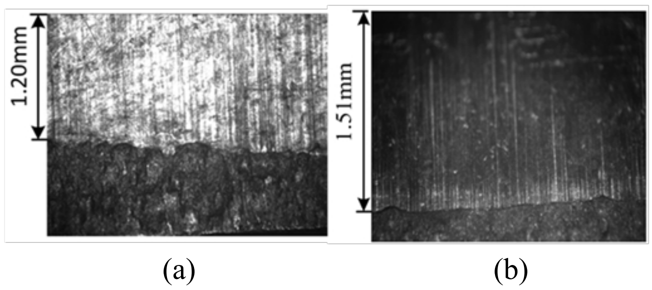

Fig.17. Cutting surface of part: (a) Process parameters before improvement and (b) Improved process parameters.

Optimized experimental and simulation results are shown in Table 5. It can be seen that the error of maximum blanking force is 2.05% and that of bright band length is 3.97% after optimization. Both of the errors are within the allowable range, which proves the reliability of the above modeling.

TABLE 5.
COMPARISON OF OPTIMIZED EXPERIMENT AND SIMULATION RESULTS

Location	The actual value	Simulation value	Error
Maximum blanking force (KN)	58.6	58.48	2.05%
Length of bright band (mm)	1.51	1.45	3.97%

The experiment is carried out with the original process parameters, and the blanking clearance is set as 0.18mm, the blanking speed is set at 4mm/s and the radius of fillet of punch edge is set as 0.5mm. The experiment is carried out with the optimized process parameters, i.e. blanking clearance 0.15mm, radius of fillet of punch edge 0.4mm and punching speed 5mm/s. Two groups of parameters were manufactured together for 4 hours to compare the number of experimental samples.

TABLE 5.

COMPARISON OF ACTUAL PRODUCTION BEFORE AND AFTER OPTIMIZATION

Group	1	2
Blanking clearance x_1 (mm)	0.18	0.15
Punch edge fillet radius x_2 (mm)	0.5	0.4
Blanking speed x_3 (r/min)	4	0.5
Time t (h)	4	4
Number y (n)	260	328
Number/ Time	65	82

V.CONCLUSIONS

In this study, the mechanical model of maximum blanking force is established by using slip line field theory, and then the theoretical formula of maximum blanking force is derived. Based on the maximum blanking force, the finite-element simulation of the blanking process of the locating plate of the circuit breaker is carried out and combined with the central composite experiment. Several process parameters are analyzed, which have a great influence on the locating plate. The optimal combination of process parameters is obtained by multi-objective optimization. Based on the optimized process parameters, the maximum blanking force is reduced from 62.7KN to 58.6KN, achieving the purpose of reducing energy loss. The length of the bright strip is increased from 1.2mm to 1.51mm, and the production efficiency is increased by 25%. This experiment verifies the rationality of the optimized process parameters, the difference between optimized simulation results and experimental results is very small, the maximum error of the test point is less than 4%, which proves that the simulation accuracy of the positioning plate blanking is high, which has certain guiding significance for optimizing the blanking process parameters.

REFERENCES

[1] Iberraken Fairouz, Medjoudj Rafik, Medjoudj Rabah, and Aissani Djamil, "Combining reliability attributes to maintenance policies to improve high-voltage oil circuit breaker performances in the case of competing risks," Proceedings of the Institution of Mechanical Engineers, vol. 229, no. 3, pp254-265, 2015.

[2] Kramer Axel, Over Daniel, Stoller Patrick, and Paul Thomas A, "Fiber-coupled LED gas sensor and its application to online monitoring of ecoefficient dielectric insulation gases in high-voltage circuit breakers," Applied optics, vol. 56, no. 15, pp4505-4512, 2017.

[3] Dai Yue, Zhang Ming, Fan Kunpeng, Pan Yuan, Yu Kexun, and Zhuang Ge, "Investigation of Series-Connected IGBTs in Fast High-Voltage Circuit Breaker," Journal of Fusion Energy, vol. 34, no. 6, pp1406-1410, 2015.

[4] I. L. Shleyfman, "Interruption of inductive load currents with high-voltage circuit breakers," Power Technology and Engineering, vol. 48, no. 1, pp71-73, 2014.

[5] Hyunwoo So, Dennis Faßmann, Hartmut Hoffmann, Roland Golle, and Mirko Schaper, "An investigation of the blanking process of the quenchable boron alloyed steel 22MnB5 before and after hot stamping process," Journal of Materials Processing Technology, vol. 212, no. 2, pp437-449, 2012.

[6] Hong Seok Choi, Byung Min Kim, Dong Hwan Kim, and Dae Cheol Ko, "Application of mechanical trimming to hot stamped 22MnB5 parts for energy saving," International Journal of Precision Engineering and Manufacturing, vol. 15, no. 6, pp1087-1093, 2014.

[7] N. A. Jaafar, A. B. Abdullah, and Z. Samad, "Effect of punching die angular clearance on punched hole quality of S275 mild steel sheet metal," International Journal of Advanced Manufacturing Technology, vol. 101, no. 5-8, pp1553-1563, 2019.

[8] Zhutao Shao, Nan Li, Jianguo Lin, and Trevor Dean, "Formability evaluation for sheet metals under hot stamping conditions by a novel biaxial testing system and a new materials model," International Journal of Mechanical Sciences, vol. 120, pp149-158, 2017.

[9] F. Akyürek, K. Yaman, and Z. Tekiner, "An experimental work on tool wear affected by dies clearance and punch hardness," Arabian Journal for Science and Engineering, vol. 42, no. 11, pp4683-4692, 2017.

[10] Satoshi Kitayama, and Shohei Yamada, "Simultaneous optimization of blank shape and variable blank holder force of front side member manufacturing by deep drawing," The International Journal of Advanced Manufacturing Technology, vol. 291, no. 1-4, pp1381-1390, 2017.

[11] Ming Li, "Micromechanisms of Deformation and Fracture in Shearing Aluminum Alloy Sheet," Journal of Mechanical Science, vol. 42, no. 5, pp907-923, 2000.

[12] N. A. Jaafar, A. B. Abdullah, and Z. Samad, "Effect of punching die angular clearance on punched hole quality of S275 mild steel sheet metal," International journal of advanced manufacturing technology, vol. 101, no. 5-8, pp1553-1563, 2019.

[13] Nobuo Hatanaka, Katsuhiko Yamaguchi, Norio Takakura, and Takasi Iizuka, "Simulation of sheared edge formation process in blanking of sheet metals," Journal of Materials Processing Technology, vol. 140, no. 1-3, pp628-634, 2003.

[14] Hong Seok Choi, Byung Min Kim, Dong Hwan Kim, and Dae Cheol Ko, "Effect of clearance and inclined angle on sheared edge and tool failure in trimming of DP980 sheet," Journal of Mechanical Science and Technology, vol. 28, no. 6, pp2319-2328, 2014.

[15] Q. B. Le, J. A. Devries, S. F. Golovashchenko, and J. F. Bonnen, "Analysis of sheared edge formability of aluminum," Journal of Materials Processing Technology, vol. 214, no. 4, pp876-891, 2014.

[16] X. H. Hu, K. S. Choi, X. Sun, and S. F. Golovashchenko, "Edge Fracture Prediction of Traditional and Advanced Trimming Processes for AA6111-T4 Sheets," Journal of Manufacturing Science and Engineering, vol. 136, no. 2, pp021016, 2014.

[17] Seunghyeon Cheon, and Naksoo Kim, "Prediction of tool wear in the blanking process using updated geometry," Wear, vol. 352-353, pp160-170, 2016.

[18] Zafer Tekine, Muammer Nalbant, and Hakan Gunln, "An experimental study for the different clearances on burr, smooth-sheared and blanking force on aluminium sheet metal," Materials and Design, vol. 27, no. 10, pp1134 -1138, 2006.

[19] Cristian Canales, Philippe Bussetta, and Jean-Philippe Ponthot, "On the numerical simulation of sheet metal blanking process," International journal of materlal forming, vol. 10, no. 1, pp55-71, 2017.

[20] Cavusoglu Onur, and Gurun Hakan, "The Relationship of burr height and blanking force with clearance in the blanking process of AA5754 aluminium alloy," Transactions of Famena, vol. 41, no. 1, pp55-62, 2017.

[21] Seunghyeon Cheon, and Naksoo Kim, "Prediction of tool wear in the blanking process using updated geometry," Wear, vol. 352-353, pp160-170, 2016.

[22] Xianguo Hu, Yourong Wang, and Hefeng Jing, "Application of oil-in-water emulsion in hot rolling process of brass sheet," Industrial Lubrication and Tribology, vol. 62, no. 4, pp224-231, 2010.

[23] Changsheng Wang, Jun Chen, Cedric Xia, Feng Ren, and Jieshi Chen, "A New Method to Calculate Threshold Values of Ductile Fracture Criteria for Advanced High-Strength Sheet Blanking," Journal of Materials Engineering and Performance, vol. 23, no. 4, pp1296-1306, 2014

[24] Xinghua Shi, Palos Ângelo Teixeira, Jing Zhang, and Carlos Guedes Soares, "Kriging response surface reliability analysis of a ship-stiffened plate with initial imperfections," Structure and Infrastructure Engineering, vol. 11, no. 11, pp1450-1465, 2015.

[25] Xiaoliang Jia, Jing Wang, Yiliang Zhang, Gongfeng Jiang, and Yanjun Zeng, "True stress and shakedown analysis of pressure vessel under repeated internal pressure," Mechanics and Industry, vol. 17, no. 4, pp410, 2016.

[26] N. Ch. Bhatra Charyulu, and Sk. Ameen Saheb, "Note on Reduction of Dimensionality for Second Order Response Surface Design Model," Communications in Statistics Theory and Methods, vol. 46, no. 7, pp3520-3525, 2017.

[27] Raj Kumar Kamaraj, Jinu Gowthami Thankachi Raghuvaran, Arul Franco Panimayam, and Haiter Lenin Allasi, "Performance and exhaust emission optimization of a dual fuel engine by response surface methodology," Energies, vol. 11, no. 12, pp3508, 2018.

[28] M. A. Sahali, I. Belaidi, and R. Serra, "New approach for robust multi-objective optimization of turning parameters using probabilistic genetic algorithm," The International Journal of Advanced Manufacturing Technology, vol. 83, no. 5-8, pp1265-1279, 2016.

[29] Jian Song, Jiang Li, Qihe Yang, Xiaomin Mao, Jian Yang, and Kai Wang, "Multi-objective optimization and its application on irrigation scheduling based on AquaCrop and NSGA-II," Journal of Hydraulic Engineering, vol. 49, no. 10, pp1284-1295, 2018.

[30] Carmine Maria Pappalardo, Adriano Gabriel Manca, and Domenico Guida, "A Combined Use of the Multibody System Approach and the Finite Element Analysis for the Structural Redesign and the Topology Optimization of the Latching Component of an Aircraft Hatch Door," IAENG International Journal of Applied Mathematics, vol. 51, no.1, pp175-191, 2021.

[31] U. Mohammed Iqbal, V. S. Senthil Kumar, and S. Gopalakannan, "Application of Response Surface Methodology in optimizing the process parameters of Twist Extrusion process for AA6061-T6 aluminum alloy," Measurement: Journal of the International Measurement Confederation, vol. 94, pp126-138, 2016.

[32] D. Anand, A. Shrivastava, and D. R. Kumar, "Size Effect on Surface Roughness of Very Thin Brass Sheets in Biaxial Stretching," Materials Today: Proceedings, vol. 18, no. 7, pp2448-2453, 2019.

[33] Espirito Santo, Isabel A. C. P, Lino Costa, and Edite M. G. P. Fernandes, "On optimizing a WWTP design using multi-objective approaches," Engineering Letters, vol. 21, no.4, pp193-202, 2013.

[34] Wenshuai Liu, Xiaomin Yao, Chaoqun Li, Mengfei Zhang, Xujia Dan, and Wenting Han, "Optimization of Configuration Parameters of Tail-sitter UAV Based on Response Surface and Genetic Algorithm," Transactions of the Chinese Society for Agricultural Machinery, vol. 50, no. 5, pp88-95, 2019.

[35] Aykut Caglar, Tekin Sahan, M. Selim Cogenli, Ayse Bayrakceken Yurtcan, Nahit Aktas, and Hilal Kivrak, "A novel Central Composite Design based response surface methodology optimization study for the synthesis of Pd/CNT direct formic acid fuel cell anode catalyst," International Journal of Hydrogen Energy, vol. 43, no. 24, pp11002-11011, 2018.

[36] Chao Lu, Liang Gao, Xinyu Li, and Peng Chen, "Energy-efficient multi-pass turning operation using multi-objective backtracking search algorithm," Journal of Cleaner Production, vol. 137, no. 20, pp1516-1531, 2016.